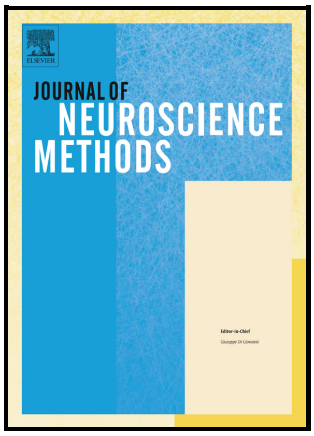

Multisite silicon probes enable simultaneous recording of spontaneous and evoked activity in multiple isolated C-fibres in rat saphenous nerve

A.C. Sales, G.W.T. Newton, A.E. Pickering, J.P. Dunham

PII: S0165-0270(21)00354-X

DOI: https://doi.org/10.1016/j.jneumeth.2021.109419

Reference: NSM109419

To appear in: *Journal of Neuroscience Methods*

Received date: 28 June 2021
Revised date: 21 October 2021
Accepted date: 11 November 2021

Please cite this article as: A.C. Sales, G.W.T. Newton, A.E. Pickering and J.P. Dunham, Multisite silicon probes enable simultaneous recording of spontaneous and evoked activity in multiple isolated C-fibres in rat saphenous nerve, *Journal of Neuroscience Methods,* (2021) doi:https://doi.org/10.1016/j.jneumeth.2021.109419

Multisite silicon probes enable simultaneous recording of spontaneous and evoked activity in multiple isolated C-fibres in rat saphenous nerve

Sales, A.C.[1], Newton, G.W.T. [1], Pickering A.E. [1,2], Dunham, J.P. [1,2]

1 - School of Physiology, Pharmacology & Neuroscience, University of Bristol, Bristol, BS8 1TD, United Kingdom

2 - Bristol Anaesthesia, Pain & Critical Care Sciences, Translational Health Sciences, Bristol Medical School, University of Bristol, BS2 8HW, United Kingdom

Corresponding Author: JPD, james.p.dunham@bristol.ac.uk

Other author email addresses: ACS, anna.sales@bristol.ac.uk; GWTN, graeme.newton@bristol.ac.uk; AEP, tony.pickering@bristol.ac.uk

Highlights

- Multisite silicon probes allow recordings of multiple C-fibres in intact nerves
- Multisite recordings significantly increase data yields
- Data visualisations enable rapid multiplexed interpretation of complex datasets
- Clustering analysis enables tracking of multiple individual fibres without electrical marking
- Axonal conduction velocities can be calculated from spontaneous activity

Abstract

Background

Recordings of electrical activity in nerves have provided valuable insights into normal function and pathological behaviours of the nervous system. Current high-resolution techniques (e.g. teased fibre recordings) typically utilise electrodes with a single recording site, capturing the activity of a single isolated neurone per recording.

New Method

We conducted proof-of-principle C-fibre recordings in the saphenous nerve of urethane-anaesthetised adult Wistar rats using 32-channel multisite silicon electrodes. Data was acquired using the OpenEphys recording system and clustered offline with Kilosort 2.5.

Results

In single recordings in 5 rats, 32 units with conduction velocities in the C-fibre range (<1m/s) were identified via constant latency responses and classified using activity dependent slowing. In two animals, 6 C-fibres (5 classified as nociceptors) were well isolated after clustering. Their activity could be tracked throughout the recording – including during periods of spontaneous activity. Axonal conduction velocities were calculated from spontaneous activity and/or low frequency electrical stimulation using only the differences in action potential latency as it propagated past multiple probe sites.

Comparison with Existing Methods

Single electrode approaches have a low data yield and generating group data for specific fibre types is challenging as it requires multiple experimental subjects and recording sessions. This is particularly true when the experimental targets are the small, unmyelinated C-fibres carrying nociceptive information.

Conclusions

We demonstrate that multisite recordings can greatly increase experimental yields and enhance fibre identification. The approach is of particular utility when coupled with clustering analysis. Multisite probes and analysis approaches constitute a valuable new toolbox for researchers studying the peripheral nervous system.

Keywords

- Peripheral nervous system
- Multisite probes
- Nociception
- C-Fibers
- Clustering

Acknowledgements

Funding sources

This work was supported by Versus Arthritis, grant reference 22487. JPD is supported by a Clinical Lecturers Starter Grant from the Academy of Medical Sciences. GWTN is supported by a BBSRC Collaborative Training Partnership Doctoral Studentship with the University of Bristol and Eli Lilly, BBSCR grant reference BB/T508342/1.

Introduction

Pioneering work in the late 1950s and 1960s established techniques to make unitary recordings from single C-fibre sensory afferents innervating the skin of experimental animals (Bessou and Perl, 1969; Iggo, 1960). These experiments built on earlier multi-fibre recording approaches and established the existence of nociceptive C-fibre afferents which responded preferentially to noxious stimulation (Bessou and Perl, 1969; Iggo, 1960) .

These developments have been extended with the advent of microneurography, enabling equivalent recordings in humans with simultaneous psychophysical measurements (see Vallbo (2018a) for review). Further refinements have included: the 'marking technique' to overcome issues of low signal to noise(Schmidt et al., 1995; Torebjork and Hallin, 1974); An *ex-vivo* preparation which provides greater flexibility for pharmacological manipulation (Reeh, 1986; Zimmermann et al., 2009); and the observation that specific sub populations of nociceptors alter their conduction velocity to differing extents during high frequency stimulation(Gee et al., 1996; Serra et al., 2004; Weidner et al., 1999) .

Despite these advances, the basic principle of using a single active electrode to make a differential recording in the peripheral nervous system, either in animals or people, has not changed in nearly 70 years (Vallbo, 2018b). In contrast, multi-contact electrodes have been widely adopted to make recordings in the central nervous system (for summary see (Steinmetz et al., 2018)). Multi-contact electrodes offer substantial advantages including greatly increased data yields and consequently reduced experimental times. With multi-contact electrodes, action potentials originating from a single cell can be recorded by more than one contact. This increased dimensionality in the data enables 'clustering' of events synchronised in time and with consistent morphology across contacts, facilitating the isolation of activity from individual units (Quian Quiroga, 2012; Rey et al., 2015). This principle has successfully formed the core of many 'clustering' algorithms commonly used to analyse recordings in the central nervous system (e.g. (Buccino et al., 2020; Chung et al., 2017; Fujisawa et al., 2008; Pachitariu et al., 2016; Quiroga et al., 2004; Souza et al., 2019)).

These features could also be advantageous for nerve recordings -but there are multiple barriers to using multi-contact electrodes in the periphery. These include the fact that most multi-contact electrodes are constructed on a silicon wafer and are therefore too brittle to be passed through the skin and connective tissue, the relatively high cost of each probe (~$1000) and the lack of off-the-shelf software optimised for viewing and processing data recorded from peripheral nerves. Notwithstanding these challenges, we set out to conduct experiments to test whether commercially available multi-contact electrodes can be used to make recordings in the peripheral nervous system,

and whether, with appropriate algorithms for data processing, “single fibre” level data can be collected during “multi-fibre” recordings. We also test the hypothesis that clustering approaches can allow spontaneous activity of multiple individually identified units to be tracked over time without the need for marking techniques. The introduction of such techniques has the potential to greatly improve experimental yields and facilitate targeting of specific fibre types.

Materials and methods

All experiments and procedures conformed to the UK Animals (Scientific Procedures) Act 1986 and were approved by the University of Bristol Animal Welfare and Ethical Review Body. Rats were group housed, with food and water available ad libitum, on a 12 hr/12 hr light/dark cycle. 5 male adult Wistar rats (weight 220-375g) were used for saphenous nerve recordings under terminal anaesthesia.

Experimental preparation

Surgery

Anaesthesia was induced using urethane (Sigma) with an initial dose of 1.5-2g/kg i.p to achieve loss of paw withdrawal reflex. The animal was placed supine on a warming mat and the medial aspect of the hind limb was shaved from knee to groin crease. A longitudinal skin incision was made to expose the saphenous nerve. A suture was inserted into the patellar ligament, passed through the skin, and tied to externally rotate the hip, allowing access to the saphenous nerve. This access was improved by fixing the plantar surface of the paw (using double sided tape, Figure 1(a)). A pool for mineral oil was constructed by attaching the skin edges, blunt dissected away from the underlying tissues, to a metal ring held in a clamp stand.

A 5mm section of the saphenous nerve was carefully freed from surrounding tissue and blood vessels by blunt dissection with fine forceps under a dissecting microscope. The neural sheath was stripped using a 30-gauge (12mm) needle bent at the tip to create a fine ‘hook’. This hook was used to catch and pull back tissue including the epineurium surrounding the nerve. This was necessary because of the fragility of the silicon probe – which is liable to bend and break if it encounters any significant resistance upon insertion. Despite this risk, this study used only one probe - which was successfully reused in each animal without any breakage. The exposed area of nerve was immersed in mineral oil to prevent drying (Figure 1b).

Probe recordings

To record neural activity, a 32 channel silicon probe (Neuronexus A1x32-Poly3-10mm-25s-177) was used in combination with a 32 channel amplifier headstage (Intan, RHD 2132, #3314). This combined headstage and A-D converter on a chip supporting 32 channels of data sampled at 30Khz each, with a gain of x192 (see https://intantech.com/products_RHD2000.html). The probe and headstage were connected using a Neuronexus headstage adaptor (#A32-OM32). Output from the probe was recorded using the OpenEphys recording system (https://open-ephys.org/). After each experiment, the probe was cleaned via 2-hour immersion in Tergazyme enzyme detergent (Sigma Aldrich, 1% concentration in distilled water), followed by 10 minutes immersion in PBS. Prior to each experiment, probe site impedances were measured using OpenEphys whilst the probe was immersed in PBS, to check that all sites were still functional (functional impedances were expected to be ~1MOhm). No sites were found to be defective during the set of 5 experiments.

The probe was held in a hydraulic micromanipulator (Narishige) and the nerve was approached at a shallow angle (Figure 1b and c). The nerve was stabilised and taut using fine forceps holding the connective tissue sheath to avoid neural damage. The probe was then advanced slowly into the exposed nerve. Data was displayed on the Open Ephys graphical user interface during insertion, using a signal chain in which channel data was bandpass filtered (300-6000Hz) and common average referenced. When the insertion was successful, action potentials were immediately visible across multiple channels (an example of data over 7 channels is shown in Figure 1d). Typically, between 1-5 insertion attempts were needed to see unit activity.

Search technique

If units were visible on the probe, a paintbrush was used to brush the dorsal surface of the foot exploring the territory innervated by the saphenous nerve (hairy skin on medial side (Kambiz et al., 2014)) to identify the area of skin innervated by the fascicle(s) into which the recording electrode had been inserted. This is analogous to previously published techniques in rat (George et al., 2007) and human microneurography (Vallbo et al., 2018 and references therein). receptive fields. If found, unit responses to electrical stimulation were checked with a bipolar transcutaneous stimulator connected to a constant current stimulator (DS4, Digitimer, UK). The stimulator was controlled via TTLs generated from an Arduino Uno, using custom scripts to enable TTLs to be delivered at different intervals. Pulses of 0.5mA and 0.5ms duration were used to evoke responses from axon terminals in putative receptive fields.

Recording protocol

Once one or more units were found with response latencies in the range of C-fibres (corresponding to conduction velocities of <1m/s), the bipolar electrical stimulator was fixed into place above the receptive field using a micromanipulator. The recording protocol was then started lasting approximately one hour and only one recording session was undertaken per animal. The protocol was designed to allow classification of units via activity dependent slowing (ADS) of conduction velocity during high frequency activity (stimulated electrically), in addition to recording spontaneous activity and responses to light touch, mechanical stimulation, before and after application of the TRPA1 agonist cinnamaldehyde:

1. 10 minutes recording of spontaneous activity
2. Coarse thresholding of evoked responses. The stimulus current was titrated down (from 0.5 to 0.1mA, over 0.5ms) to find the lowest intensity capable of evoking reliable action potential discharge
3. A series of electrical stimuli delivered at prespecified frequencies (protocol as described by ((Obreja et al., 2010)). Specifically:
    - 20 pulses at 0.125Hz
    - 20 pulses at 0.25Hz
    - 30 pulses at 0.5Hz
    - 20 pulses at 0.25Hz
    - 2 minute resting period
    - 3 minutes stimulation at 2Hz, followed by 60 pulses at 0.25Hz.
4. Spontaneous activity recorded for 5 minutes
5. Application of sensory stimuli, consisting of gentle strokes across the receptive area with a paintbrush and mechanical stimulation with von Frey hairs (0.16g, 0.6g, 1.4g and 2g). Each stimulus was timestamped via a foot pedal which generated a TTL recorded an 'Analogue In' port on the Open Ephys board.
6. Application of cinnamaldehyde (0.5ml of 10% (v/v) in ethanol delivered from a 1ml pipette) to the skin of the dorsal surface of the hindpaw and ankle.
7. Algesic evoked ongoing activity for 15 minutes

At the end of the experiment, the distance between the probe insertion point and the receptive field was estimated using digital callipers.

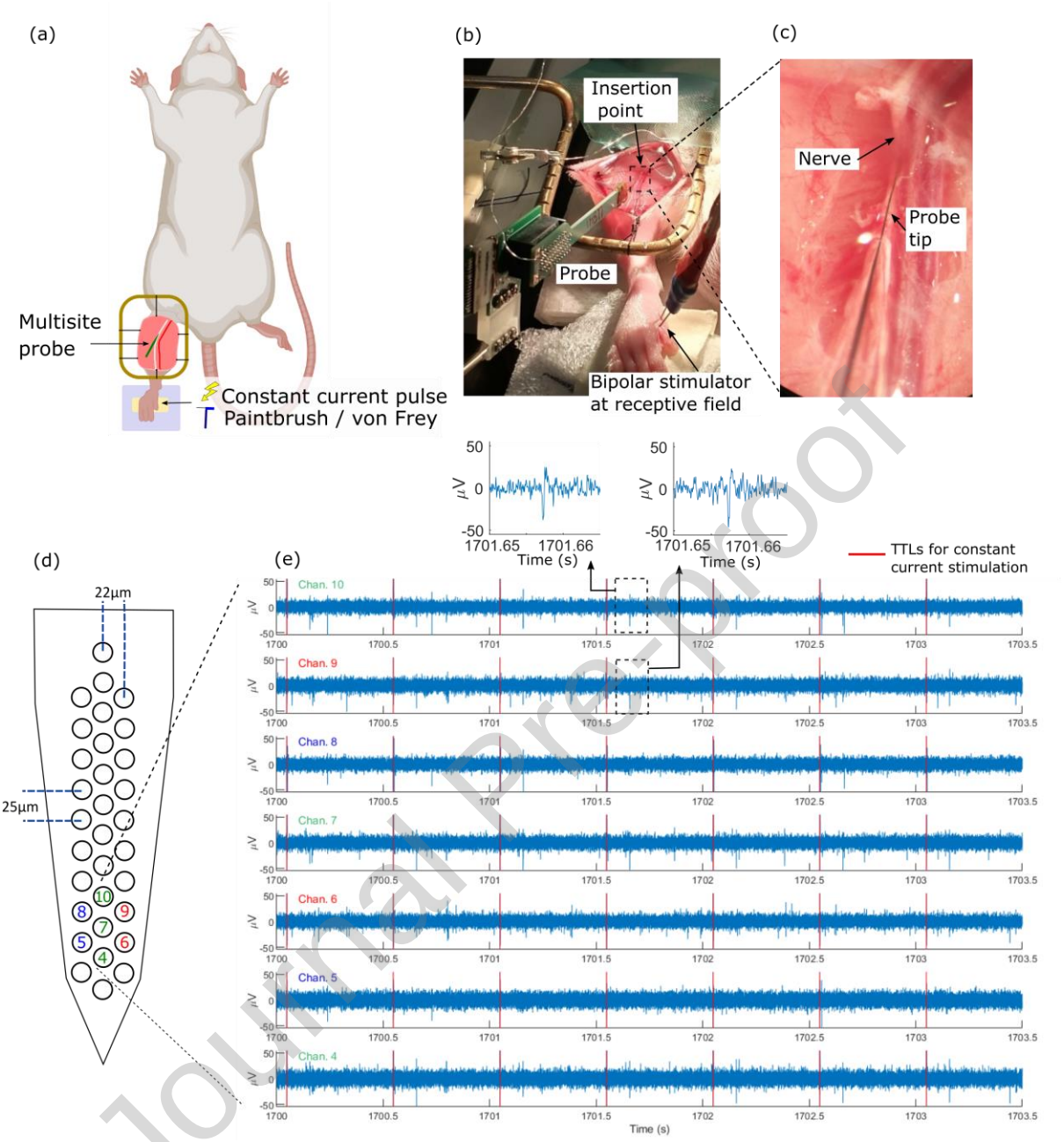

Figure 1 Overview of experimental approach. (a). Recordings were made from saphenous nerve in adult Wistar rats in combination with sensory/electrical stimulation of receptive fields (b) the approach to the nerve (c) close-up of probe insertion – a small area of nerve is freed from the surrounding tissue, de-sheathed and covered in mineral oil. The exposed nerve is then gently supported as the probe is advanced. (d) schematic of 32 site recording probe, with example of raw data gathered on a subset of channels. Individual action potentials are visible as 'spikes' in the voltage (examples shown for two spikes from channels 10 and 9). Note the difference in spiking activity between channels only 36µm apart – for example, whilst a spike is clearly visible on channels 9 and 10 (enlarged spikes at top of (e)) there is no sign of the same event on channel 8. This illustrates the ease with which units may be missed in single channel recordings. Here channels in the right column of channels (9 and 6, in red) and the centre column (10, 7, 4, in green) 'see' more activity than those on the left column (8 and 5, in blue)

Data analysis

Probe-based and latency-based heatmaps

All 32 channels of bandpass filtered (300-6000Hz) and common average referenced data were saved from OpenEphys. Spatial activity heat maps were created to aid visualisation of the location on the probe of possible action potentials during electrical stimulation. To generate these probe-based heatmaps (Figure 2a and 2c), on each channel, a window of data 300ms long was extracted around each of the first 25 current pulses delivered at 0.25Hz (using events from the first section of the Obreja protocol). For each 300ms section of data, the times of possible action potentials were extracted by first selecting points above a threshold of 3 times the standard deviation of the data; peaks in the thresholded data were then identified using the MATLAB function 'findpeaks'. The number of spikes in each 1ms bin over the window was then counted. Spikes detected in the first 5ms of the window were discounted due to the presence of the stimulus artefact (see Supplementary Figure 1). For each channel, spike counts were averaged over the 25 stimuli. The resulting matrix of spike counts over time (columns) for each channel (rows) was then displayed as a heatmap using MATLAB's 'imagesc' function. Thus the 'hotter' the colour, the greater the number of possible action potentials detected on that channel.

Trial to trial latency-based heatmaps (Figure 2b and d) were generated using a similar approach. A 300ms window of data were extracted following each of the 2Hz electrical stimuli. In each window of data, mean values of voltage were calculated over 0.1ms bins. The first 5ms were again excluded due to the presence of stimulus artefact. Binned mean voltage values were then summed over channels, and the resulting 2-D matrix (time vs stimulus number) was displayed using 'imagesc'. This approach allowed the data to be visualised at an expanded temporal resolution and enabling single trial by trial variation to be seen by collapsing the spatial information from the multiple sites to display a single aggregate voltage. This was especially useful when attempting to distinguish multiple C-fibres with similar baseline conduction velocities but differing degrees of activity dependent slowing. Response latencies at the beginning and end of the period of 2Hz electrical stimulation were extracted for each clearly visible track using MATLAB's data 'brush', to return data points from figures. Where tracks were not visible throughout the entire 3 minutes, the latencies were estimated from the start/end of the track section that could be identified. Specific examples are shown in Figure 2b, where the start/end points used for estimation of activity dependent slowing are marked. Units were classified as C-nociceptors if conduction velocity slowed by >10% during 3 minutes of 2Hz stimulation, (Hoffmann et al., 2015; Obreja et al., 2010; Serra et al., 2012).

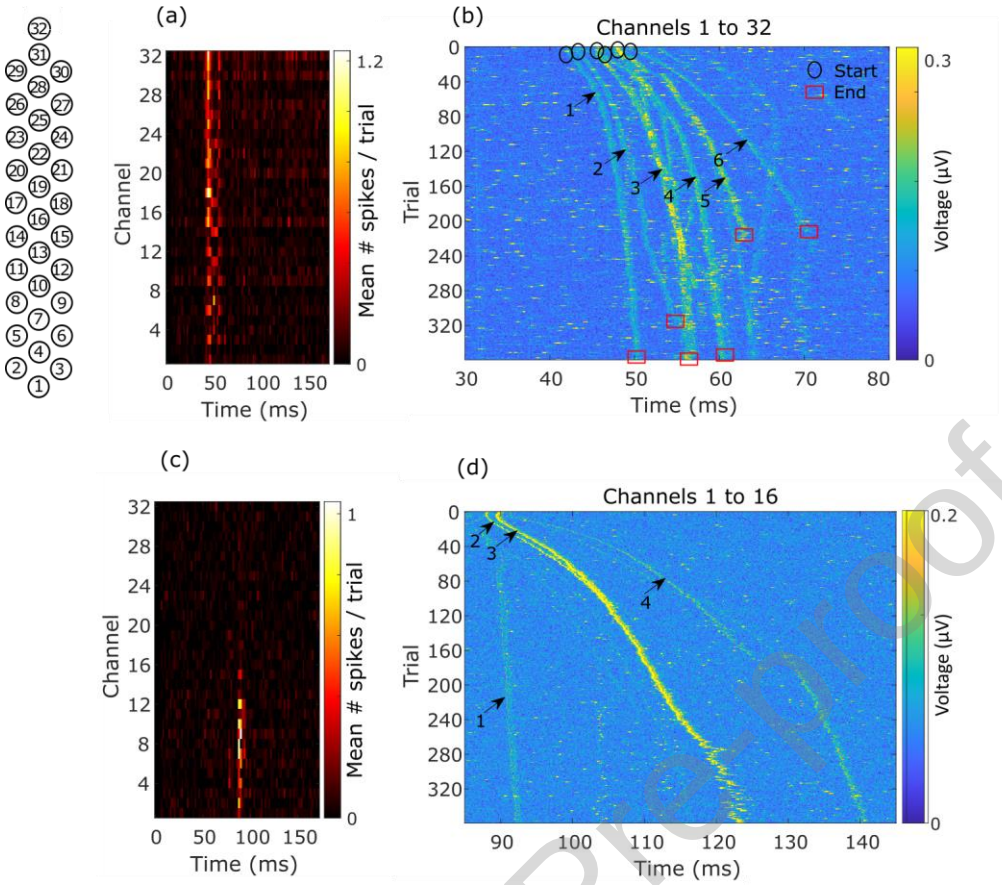

Figure 2 Heatmap views of evoked unit activity data for two example experiments (rat #5 upper, rat #3 lower). Left, (a) and (c), spatial activity heatmaps showing the location of significant spiking activity on the probe, using 25 electrical stimulations delivered at 0.25Hz during the initial phase of the electrical stimulation protocol. This visualization can also be used to estimate the conduction velocity for visible units. Right (b) and (d), trial by trial latency variation heatmaps during 2Hz stimulation in the same experiments, showing multiple candidate C-nociceptor/C-non-nociceptor fibres on individual recordings (numbered). In this view, data is averaged over the active channels (i.e. those channels shown in (a) or (c) which exhibit units with constant latency responses within the time period of interest corresponding to C-fibre conduction velocity). In this heatmap, the data is binned with a 0.1ms width to gain a high resolution view of the slowing of different units. This allows an estimate to be made of the number of different units present with conduction velocities in the C-fibre range, and their degree of activity dependent slowing during 2Hz stimulation (indicating whether the units are C-nociceptors if slowing is >10%, see Supplementary Table 1 / Supplementary Figure 2 for analysis of all heatmaps)

Clustering

An overview of the data processing pipeline is provided in Figure 3a. Clustering was undertaken using the Kilosort2.5 algorithm ((Pachitariu et al., 2016), https://github.com/MouseLand/Kilosort). This algorithm was selected because of its ability to deal with 'overlapping' spikes (that is, spikes from different units occurring at similar times) and improved capacity to correct for probe

movement relative to the nerve ('drift'). To prevent errors arising from the stimulus artefacts, values in the 5ms around each TTL (from -1ms before the TTL to 3ms after) were set to the mean voltage value over the entire recording using a custom MATLAB script. The 32 individual channels of edited data were then compiled into a single binary file and read into Kilosort. Default parameters were used, except for:

- the minimum firing rate used to define an acceptable cluster (set to ks.ops.minFR=0.0005) equivalent to a unit firing every 30 minutes and intended to account for units which were silent except for response to a single aspect of the stimulation protocol
- ks.ops.throw_out_channels, set to zero to force the algorithm to consider all channels, even if only recording sparse activity
- ks.ops.AUCsplit, set to 0.75 to allow a sightly looser criterion for splitting clusters.
- The batch size (ks.ops.NT) was also increased to avoid memory problems when clustering on a laptop.
- The spike extraction threshold (ks.ops.spkTh) was either set to -5 or -6, depending on the signal to noise ratio.

Output from Kilosort was visualised in PHY2 (https://github.com/cortex-lab/phy/) and curated – allowing splitting/merging of clusters as necessary. Only those clusters with a physiologically appropriate waveform and evidence of a refractory 'valley' in the autocorrelogram were marked as 'good' (considered as candidate single units, see Figure 3c,e for examples). Some other (non-isolated) clusters in which responses to electrical stimulation were seen were further investigated to better understand why the algorithm was unable to separate out individual fibres (Supplementary Figure 4). Conversely, pairs of clusters with identical waveforms and refractory valleys in their cross-correlograms were merged in PHY where appropriate (as described in guidance at https://phy.readthedocs.io/en/latest/sorting_user_guide/)

All further analysis was performed in MATLAB R2020b using custom scripts and the openEphys analysis scripts provided at https://github.com/open-ephys/analysis-tools. Spike times for clusters were imported to MATLAB along with the times of all event TTLs and pedal markers for sensory stimulation, for visualisation and analysis. 'Good' (i.e. isolated) units were further validated by ensuring that there was only a single 'trace' of constant latency responses/activity dependent slowing during the electrical stimulation protocol (Figure 3b), and that the waveform during electrical activity matched the waveform recorded at other times in the recording (example shown in Figure 3d, this ensures that the clustering software has not erroneously combined two separate units, one of which only fires during electrical stimulation).

Analysis of isolated clustered units

Auto and cross correlograms shown in Figure 3 were plotted in MATLAB (to recreate the output seen in PHY) by allocating the spikes into 2ms bins over the entire period of the recording, and then calculating auto and cross correlations using the MATLAB function 'xcorr'.

The action potential waveforms for each cluster were extracted from the raw data using the PHY helper function 'getwaveforms', which returns waveforms from the raw data binary file using specified spike times and cluster identification numbers generated in the PHY output. This was adapted to return both the waveform standard deviations and means for all channels for the specified spike times. Spikes were considered as likely generated by the electrical stimulation if they occurred within 150ms.

Activity dependent slowing for clustered data (i.e. for isolated units) was calculated by taking the first 5 and last 5 spike times during the 2Hz stimulation for each cluster, and calculating the latency change between the mean of the two sets (in addition to the slowing estimated from heatmap plots).

The histograms of spiking activity shown in Figure 4 (a) and (c) were generated by allocating spikes into 1s bins and plotting relative to event markers for sensory stimulation. Bar charts for spiking activity (Figure 4b) were generated by calculating the number of spikes per second during each event (e.g. a von Frey hair applied to a receptive field). Multiple trials were performed for each event type; these were averaged to produce a mean firing rate for each event type for each cluster. Firing rates were compared using a 1-way ANOVA followed by a Tukey-Kramer correction for multiple comparisons. Changes in firing due to cinnamaldehyde were analysed by calculating the spike count over 1s bins in the 60 seconds before and after application. The significance of changes were assessed using a Wilcoxon ranksum test.

To estimate the conduction velocity and direction of travel, the mean spike waveform for each cluster was calculated and plotted for each channel (probe site) over a time period which included spontaneous activity, and responses to electrical stimulation at or below 0.5Hz. Electrical stimulation was included to enable calculations for units that were otherwise silent without the electrical stimulation. This would not otherwise have been necessary, as demonstrated by conduction velocity estimations for putative sympathetic efferents (see Figure 5). A subset of channels were manually selected where the morphology of the waveform was consistent, and either the trough or the peak of the action potential was clearly visible (between 8-11 channels were used). The time at which this feature appeared was logged for each channel, producing a matrix of time differences between each pair of channels. The distance in the horizontal and vertical directions (relative to the probe)

between each channel pair was also calculated, allowing a table of estimated speeds in either direction to be produced. The mean speed in the horizontal and vertical direction was then calculated, allowing estimation of the overall vector direction of travel of the propagating action potential and the absolute magnitude of its speed.

Results

The multisite probe recordings were stable over the duration of the stimulation protocol (~1 hour) in all five animals. Analysis of the recordings identified 32 fibres that had conduction velocities in the C-fibre range, calculated from their constant latency responses to 0.25Hz stimulation (Figure 2). Of those, 20 (63%) exhibited activity dependent slowing of >10% during 2Hz electrical stimulation, and were therefore classified as nociceptors (Hoffmann et al., 2015; Serra et al., 2012) (see Supplementary Table 1).

Clustering was attempted on all datasets (Figure 3a). Of the 5 recordings, 2 yielded isolated C-fibres (see examples in Figure 3b-e). These were the recordings from rat #3 (4 isolated units, Figure 3) and #4 (2 isolated units, Supplementary Figure 3). In the recording from rat #3, 3 of 4 fibres displayed activity dependent slowing of >10% during electrical stimulation at 2Hz and were therefore classified as C-nociceptors (Table 1).

Table 1 Classification of clustered C-fibres for recording from Rat #3. Spike numbers are defined relative to the start of the 2Hz stimulation such that L_{start}= mean latency of first 5 spikes of 2Hz period, L_{end}= latency of final 5 spikes of 2Hz period.

Fibre #	L_{start} (ms)	Initial conduction velocity (m/s)	L_{end}(ms)	% slowing
1	89.8	0.52	123.1	37.1
2	85.2	0.55	92.2	8.2
3	88.1	0.53	105.8	20.1
4	94.2	0.50	140.3	49.0

Further investigation of the clustering process suggested that the extraction of spikes in Kilosort was accurate (Supplementary Figure 4a), with spiking raster plots generated from all clusters in the processed data matching that in the raw data heatmaps. However, in recordings from rats #1, #2 and #5, clusters containing multiple C-fibres (i.e. with a response to electrical stimulation of conduction velocity <1m/s) were not 'cluster-able' into single units (no trough was seen in the autocorrelogram, examples shown in Supplementary Figure 4b).

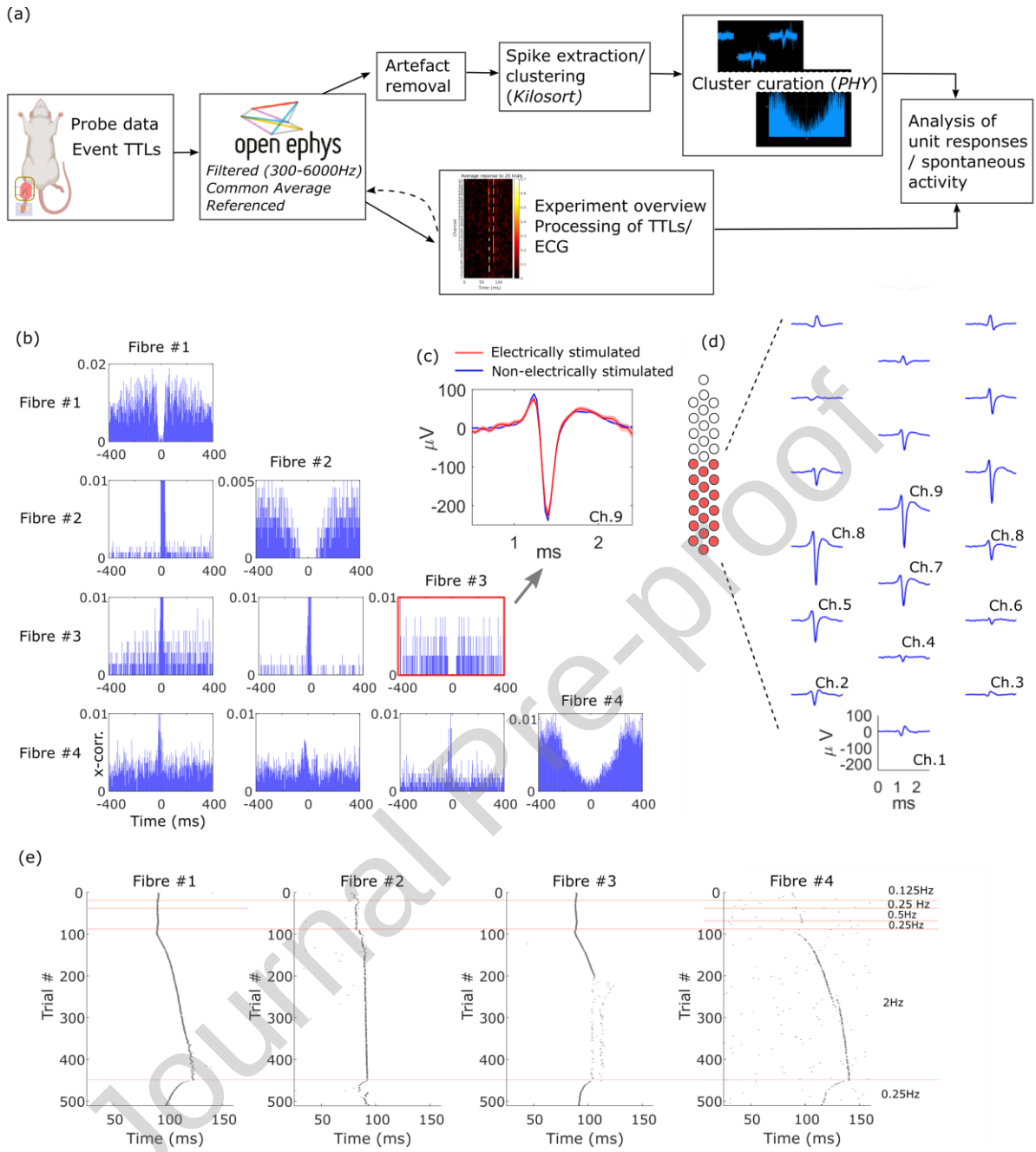

Figure 3 Overview of data analysis strategy including clustering (a) The data processing pipeline for clustering. (b) After clustering, units were classified as single-unit, 'well isolated' recordings only if the autocorrelogram showed a clear 'refractory valley' around t=0 which is not present in the cross-correlogram with other units. Data shown is for a recording (rat #3) which successfully clustered into four distinct c-fibres. Note the high correlation at t=0 in cross-correlograms, which reflects synchronized spiking caused by electrical/sensory stimulation. (c) To be classified as 'single', units were also required to present waveforms that were the same in shape whether activity is electrically (red trace) or non-electrically (blue trace) evoked. Example shown is for channel with the largest visible waveform, here, this is channel 9. (d) In well isolated units, a physiologically-appropriate average waveform across multiple channels can be plotted. (e) For the

same example recording, the latency of the action potential of each fibre during the electrical stimulation protocol is shown

The full potential of the multisite technique is illustrated more clearly by the analysis of clustered data for periods when no electrical stimulation was used. The 4 isolated units from rat #3 could be tracked throughout the recording, and individual firing responses to mechanical pressure at the receptive field with von Frey hairs, gentle stroking with paintbrush and application of cinnamaldehyde were analysed (Figure 4a-d). Based on their increasing response to mechanical pressure from von Frey hairs, Fibres 1, 3 and 4 were classified as C-mechanosensitive afferents. These fibres all showed large persistent increase in their firing rates with the application of the TRPA1 agonist cinnamaldehyde indicating that they were a class of fibre involved in the allogenic action of this agent. Fibre 2 was tentatively classified as a C-low threshold mechanoreceptor (C-LTM), due to the low degree of ADS (Watkins et al., 2017), response to brush and lack of response to von Frey or cinnamaldehyde. This clustering approach enables true firing rates to be measured, as opposed to the implied firing rates derived from the 'marking' technique (in which electrical stimulation is delivered concurrently with mechanical/thermal stimulation, and responsive units are identified by their transiently reduced conduction velocity when responding to both stimuli within a short time).

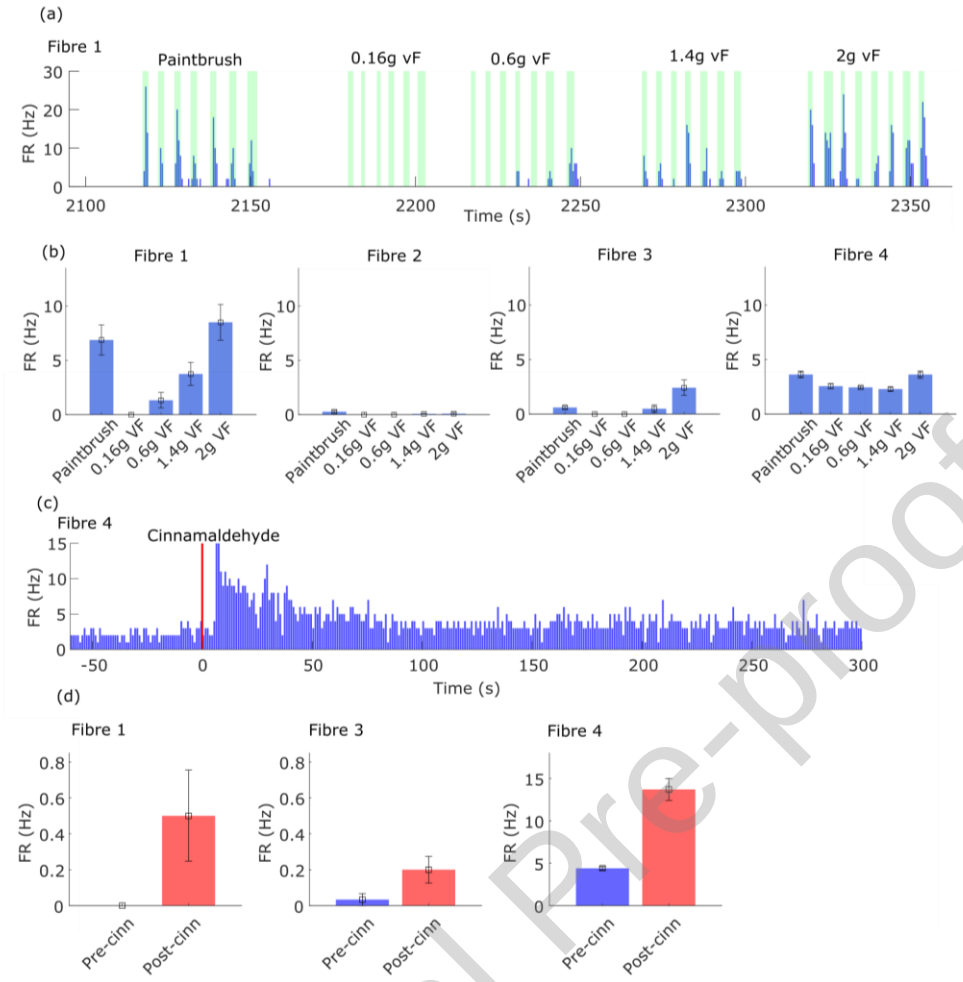

Figure 4 Responses of individual primary afferents to sensory stimuli. (a) Example of spiking responses of Fibre 1 during paintbrush/von Frey stimulation (b) summary results for all units over the same events (c) example of response to topical cinnamaldehyde from Fibre 4 (d) summary results for fibres 1, 3 and 4, counting spikes in 2s bins for 60 before and after cinnamaldehyde was applied. Fibre 2 was silent before and after cinnamaldehyde application and is not shown.

In units identified by clustering, small differences in the timing of action potentials seen on different channels were used to estimate the conduction velocity and direction of propagation of activity in individual c-fibres (Figure 5). This was achieved by selecting a subset of channels on which the same action potential feature was clearly visible (example shown in Figure 5(a), in which the action potential trough is used as the tracked feature). The time difference between the appearance of the feature on multiple channels can then be extracted. In combination with the known distance between probe channel locations, this information can then be used to estimate the conduction velocity and direction of travel - i.e. if the APs are travelling toward the spinal cord (afferent) or towards the periphery (efferent, Figure 5(c))

For the units recorded in rat #3, this technique was able to provide a reasonable match to conduction velocities calculated via latency tracking – and would also have classified all units unambiguously as slowly conducting, unmyelinated fibres (supplementary table 1). The calculated trajectory of the action potential across the probe was also consistent with heatmap analysis (Figure 2(c)) – showing fibres travelling across the lower set of probe sites. Significantly, this analysis requires no stimulation at the receptive field, and may be performed using spontaneous activity alone (Figure 5(c).

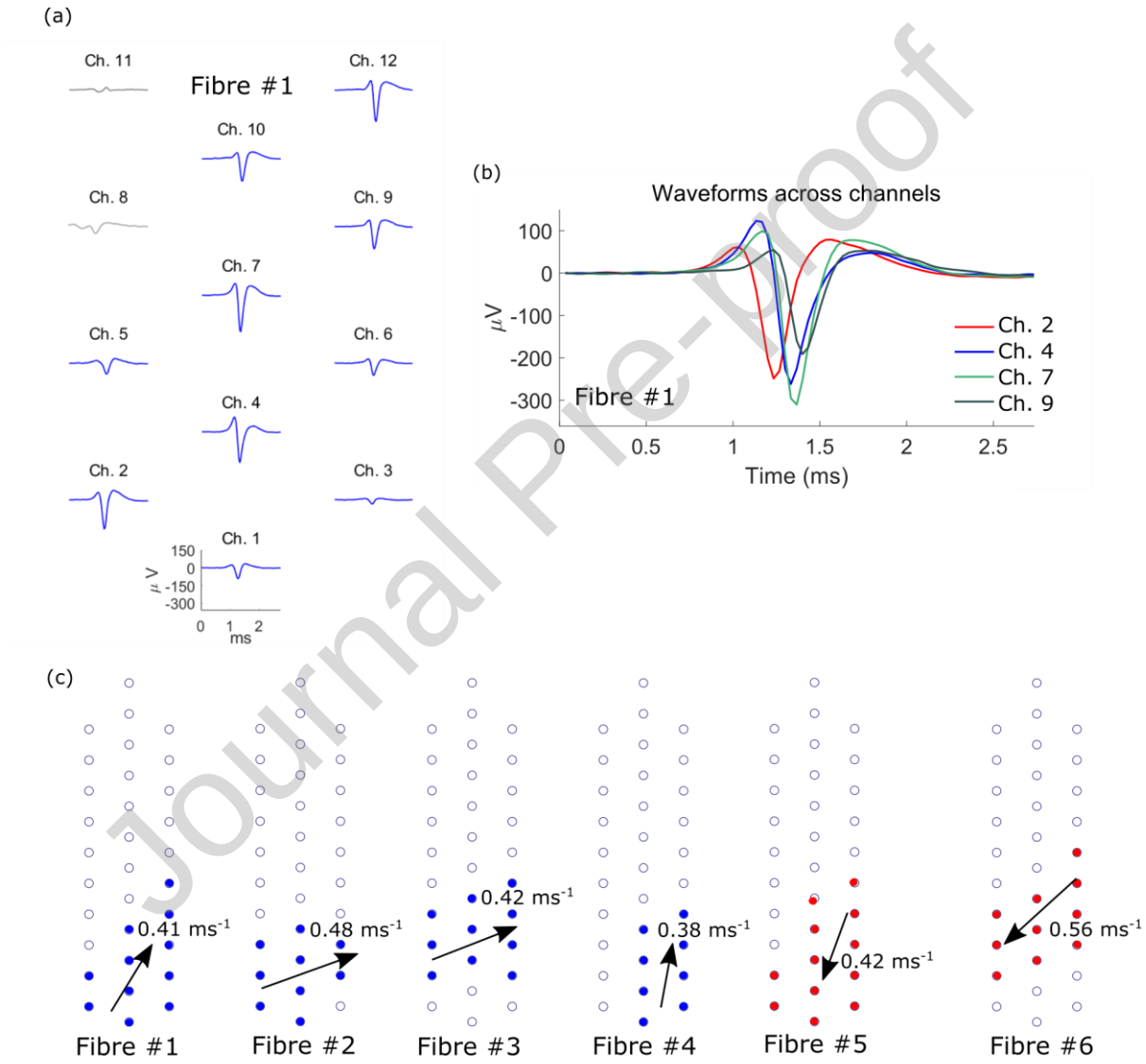

Figure 5 Determining the conduction velocity and direction of travel relative to the probe. Figures (a) and (b) show Fibre #1 (for the same experiment shown in Figure 4) (a) The trough of the action potential is clearly identifiable on channels 1-7, 9, 10, and 12. (b) When mean waveforms are overlaid on 4 example channels, it is clear that there is a time difference between the appearance of the trough on the different channels as the waveform moves left to right across the probe (c) this information can be used to calculate the conduction velocity relative to the probe. Coloured channels shown in (c) are those used in the calculation of conduction

velocity. Fibres 5 and 6 were well isolated units from the same experiment (rat #3) and fired consistently throughout the recording at 0-4Hz. They did not respond to electrical / sensory stimulation at the receptive fields identified for Fibres 1-4. Based on spontaneous activity, these action potentials were seen to be traveling in the opposite (i.e. efferent) direction, with a velocity consistent with unmyelinated fibres. We hypothesise that these are sympathetic efferents, recorded concurrently with the C-fibre afferents, and which are found within the rat saphenous nerve, Gee et al (1996).

Discussion

This study demonstrates the advantages of using multi-contact recordings in the peripheral nervous system. In order to accomplish this, we combined multiple aspects of earlier approaches. The nerve is prepared initially in the same way as for a teased fibre experiment - though it is always left intact. The electrode is inserted in a manner analogous to microneurography - but directly into the prepared nerve and not percutaneously. Standard methods in unit classification were then employed, including calculation of conduction latency to low frequency stimulation, activity dependent slowing in response to high frequency stimulation and responses to increasing mechanical pressures and application of an algesic compound, cinnamaldehyde. These approaches were combined with analytical techniques more commonly used in the central nervous system, including clustering algorithms and measures of unit isolation (e.g. assessment of refractory periods in auto-correlograms). These established analysis techniques were then extended: enabling extraction of firing rates for individual C-fibres during multiunit recordings and derivation of conduction velocity and direction in the absence of peripheral electrical stimulation. These approaches enabled algesic-evoked ongoing activity to be measured at single unit resolution in multi-contact recordings without the need to use the marking technique. A potential use of this technique would be in the assessment of spontaneous activity in pain states before and after therapeutic intervention.

In 5, one-hour, experiments, the activity of 32 C-fibres were recorded, a discovery rate of 6.4 fibres per rat with between 3 and 12 fibres recorded simultaneously in each experiment (figure 2 and supplementary figure 2). Using a comparable *in vivo* microneurography approach in the rat, mostly utilising the marking technique and activity dependent slowing to classify fibres, George et al (2007) reported recording 76 units in a sample of 28 animals – a rate of 2.7 fibres per rat, which is approximately half the rate we achieve and in which separate recordings were required to investigate the majority of single fibres– a significantly more time-consuming approach.

Furthermore, we demonstrate, in one recording, isolated activity from 4 C-fibres being tracked throughout electrical and naturalistic stimulation. This data quality is comparable to that obtained

via the teased fibre technique, showing how the use of multi-contact recordings enables the properties of multiple single fibres to be investigated simultaneously (and without the need for electrical 'marking'). The yield of 6 clustered C-units from 5 rats is analogous to the teased fibre approach, for example, Gee et al (1996) analysed 61 C-fibres collected across experiments in 52 rats, a rate of just over 1 fibre per animal. Multi-contact recordings enable this data to be collected much more efficiently. It is our experience that identifying C-units via the teased fibre approach can take up to 4 or 5 hours, in comparison to approximately 1 hour in these experiments.

As well as increasing the amount of data available to researchers, application of the multisite approach also contributes towards the goal of reducing the number of animals used in research, and the time each animal spends in each experiment (an effort supported in the UK by the National Centre for the Replacement, Refinement and Reduction of Animals in Research (https://www.nc3rs.org.uk)).

Clustering also enabled the use of multisite information to estimate the conduction velocity of different fibres – the first time this has been possible in an intact nerve *in vivo* without latency tracking (i.e. measurement of the latency between stimulation at the receptive field and recording of an action potential downstream). In addition to assisting with afferent fibre identification, this technique also offers the possibility of differentiating efferent from afferent fibres, purely on the basis of direction of action potential propagation. Novel probe site geometries are likely to improve the accuracy of this technique. For example, a larger square grid of sites, perhaps even more closely spaced that the probe used in this study (sites < 25µm apart) would provide a greater 'sampling' of action potentials in both the horizontal and vertical directions.

An additional advantage of the multisite recording approach is to be able to simultaneously record the change in firing activity across multiple neurons to the application of a sensitising agent (e.g. cinnamaldehyde). This allows the separation of neurons expressing TRPA1 (showing an increase in their firing) from those which do not. This greatly extends the possible methods for classification of primary afferents to include expression of transducer molecules and also allows quantitative assessment of the selectivity and potency of specific agonists/antagonists and their effect on the discharge patterns and intrinsic properties of the neurons.

Conclusions

This study has demonstrated the gains available through multisite recordings in intact nerves. However, in order to fully exploit this technology, we also identify the following challenges which could be profitably addressed in further work:

- **Clustering algorithms:** the inability of the clustering package (Kilosort) to isolate C-fibres in 3 of the 5 recordings is a significant current limitation and poses a particular hurdle (although it is notable that conventional latency tracking techniques could still be used for the data on any of the 32 channels in the recording). Recordings which could not be clustered were also those with the highest number of fibres (see heatmaps in Figure 2(a) and Supplementary Figure 2(a) and (b)). It is possible that the larger number of units with similar firing times and waveforms could not be adequately distinguished by the algorithm using its existing criteria of spike times and morphologies. However, in peripheral nervous system recordings, there is potential to utilise other 'features' of individual units in order to assist clustering. These include user defined templates based on constant latency responses (i.e. 'picking out' spikes clearly from a single fibre during electrical stimulation and using the waveforms to define a template). As shown in Figure 5, the passage of individual spikes across the probe may also allow the conduction velocity of action potentials to be determined, potentially providing another way of isolating fibres. The development of algorithms able to incorporate these features may increase the success rate of clustering for peripheral nerve data. Exploration of novel probe geometries – including those with higher numbers of sites in a grid layout, as discussed above – may also assist with clustering. The incorporation of measures of quality sorting values (such as isolation distance), after curation, would also be a useful future development.
- **Probe fragility**: we have demonstrated that it is possible to record C-fibres in intact nerves even without a sharp, mechanically robust electrode. However, commercially available silicon probes intended for brain recordings are fragile. The nerve must be carefully prepared to avoid damage to the probe – and a high level of care is needed when the probe is inserted. The creation of a rigid and robust multisite probe with the capability to penetrate an intact nerve would simplify the technique described here and reduce the chances of breakage (and associated cost)
- **Bespoke software:** data from multiple channels can be challenging to interpret during the course of a typical experiment (typically a 32 channel version of the view shown in Figure 1e). We have demonstrated 'heatmap' approaches for visualising responses of multiple fibres to electrical stimulation. Open access software packages such as OpenEphys provide a relatively straightforward avenue for the implementation of such visualisations. When implemented in real-time, we anticipate that these additions will be vital for helping peripheral nerve researchers interpret the large amount of data that multi-contact

electrodes can generate, allowing easier decision making about probe placement and commencement of recording protocols.

In summary, the use of multisite probe technology has the potential to facilitate progress in any nerve where the simultaneous recording of many different fibres is of value - whether afferent, efferent, or both. For instance, the investigation of novel peripheral analgesics with fibre-specific actions, the comparison of responses in multiple fibres to identical sensory stimuli, or the connection between of single unit activity in the periphery to changes in the central nervous system, including EEG or LFP responses. A robust multisite probe would also be of high value in human microneurography studies – increasing data yields and increasing the chances of identifying fibres of interest in each experiment. Advances in the areas identified above will be crucial to realising this potential, and making multisite recording a standard tool for the investigation of the peripheral nervous system.

Competing Interests

The authors have no competing interests to declare.

Credit Author Statement

Anna C Sales: Conceptualization, Methodology, Software, Formal Analysis, Investigation, Data Curation, Writing: Original Draft, Writing: Review and Editing, Visualization. **Graeme WT Newton:** Investigation, Formal Analysis, Writing: Review and Editing. **Anthony E Pickering:** Conceptualization, Methodology, Formal Analysis, Resources, Writing: Review and Editing, Supervision, Project Administration, Funding Acquisition. **James P Dunham:** Conceptualization, Methodology, Validation, Investigation, Formal Analysis, Resources, Writing: Original Draft, Writing: Review and Editing, Supervision, Project Administration, Funding Acquisition.

References

Bessou, P., Perl, E.R., 1969. Response of cutaneous sensory units with unmyelinated fibers to noxious stimuli. J. Neurophysiol. 32, 1025–1043. https://doi.org/10.1152/jn.1969.32.6.1025

Buccino, A.P., Hurwitz, C.L., Garcia, S., Magland, J., Siegle, J.H., Hurwitz, R., Hennig, M.H., 2020. Spikeinterface, a unified framework for spike sorting. Elife 9, 1–24. https://doi.org/10.7554/eLife.61834

Chung, J.E., Magland, J.F., Barnett, A.H., Tolosa, V.M., Tooker, A.C., Lee, K.Y., Shah, K.G., Felix, S.H., Frank, L.M., Greengard, L.F., 2017. A Fully Automated Approach to Spike Sorting. Neuron 95, 1381-1394.e6. https://doi.org/10.1016/j.neuron.2017.08.030

Fujisawa, S., Amarasingham, A., Harrison, M.T., Buzsáki, G., 2008. Behavior-dependent short-term assembly dynamics in the medial prefrontal cortex. Nat. Neurosci. 11, 823–833. https://doi.org/10.1038/nn.2134

Gee, M.D., Lynn, B., Cotsell, B., 1996. Activity-dependent slowing of conduction velocity provides a method for identifying different functional classes of C-fibre in the rat saphenous nerve. Neuroscience 73, 667–675. https://doi.org/10.1016/0306-4522(96)00070-X

Hallin, R.G., Wu, G., 1998. Protocol for microneurography with concentric needle electrodes. Brain Res. Protoc. 2, 120–132. https://doi.org/10.1016/S1385-299X(97)00025-1

Hoffmann, T., De Col, R., Messlinger, K., Reeh, P.W., Weidner, C., 2015. Mice and rats differ with respect to activity-dependent slowing of conduction velocity in the saphenous peripheral nerve. Neurosci. Lett. 592, 12–16. https://doi.org/10.1016/j.neulet.2015.02.057

Iggo, A., 1960. Cutaneous mechanoreceptors with afferent C fibres. J. Physiol. 152, 337–353. https://doi.org/10.1113/jphysiol.1960.sp006491

Kambiz, S., Baas, M., Duraku, L.S., Kerver, A.L., Koning, A.H.J., Walbeehm, E.T., Ruigrok, T.J.H., 2014. Innervation mapping of the hind paw of the rat using Evans Blue extravasation, Optical Surface Mapping and CASAM. J. Neurosci. Methods 229, 15–27. https://doi.org/10.1016/j.jneumeth.2014.03.015

Marques-Smith, A., Neto, J.P., Lopes, G., Nogueira, J., Calcaterra, L., Frazão, J., Kim, D., Phillips, M.G., Dimitriadis, G., Kampff, A.R., 2018. Recording from the same neuron with high-density CMOS probes and patch-clamp: a ground-truth dataset and an experiment in collaboration. bioRxiv 370080. https://doi.org/10.1101/370080

Obreja, O., Ringkamp, M., Namer, B., Forsch, E., Klusch, A., Rukwied, R., Petersen, M., Schmelz, M., 2010. Patterns of activity-dependent conduction velocity changes differentiate classes of unmyelinated mechano-insensitive afferents including cold nociceptors, in pig and in human. Pain 148, 59–69. https://doi.org/10.1016/j.pain.2009.10.006

Pachitariu, M., Steinmetz, N., Kadir, S., Carandini, M., D., H.K., 2016. Kilosort: realtime spike-sorting for extracellular electrophysiology with hundreds of channels. bioRxiv 061481. https://doi.org/10.1101/061481

Quian Quiroga, R., 2012. Spike Sorting. Curr. Biol. https://doi.org/10.1016/j.cub.2011.11.005

Quiroga, R.Q., Nadasdy, Z., Ben-Shaul, Y., 2004. Unsupervised Spike Detection and Sorting with Wavelets and Superparamagnetic Clustering. Neural Comput. 16, 1661–1687. https://doi.org/10.1162/089976604774201631

Reeh, P.W., 1986. Sensory receptors in mammalian skin in an in vitro preparation. Neurosci. Lett. 66, 141–146. https://doi.org/10.1016/0304-3940(86)90180-1

Rey, H.G., Pedreira, C., Quian Quiroga, R., 2015. Past, present and future of spike sorting techniques. Brain Res. Bull. https://doi.org/10.1016/j.brainresbull.2015.04.007

Schmidt, R., Schmelz, M., Forster, C., Ringkamp, M., Torebjörk, E., Handwerker, H., 1995. Novel classes of responsive and unresponsive C nociceptors in human skin. J. Neurosci. 15, 333–341. https://doi.org/10.1523/jneurosci.15-01-00333.1995

Serra, J., Bostock, H., Solà, R., Aleu, J., García, E., Cokic, B., Navarro, X., Quiles, C., 2012. Microneurographic identification of spontaneous activity in C-nociceptors in neuropathic pain states in humans and rats. Pain 153, 42–55. https://doi.org/10.1016/j.pain.2011.08.015

Serra, J., Campero, M., Bostock, H., Ochoa, J., 2004. Two types of C nociceptors in human skin and their behavior in areas of capsaicin-induced secondary hyperalgesia. J. Neurophysiol. 91, 2770–2781. https://doi.org/10.1152/jn.00565.2003

Souza, B.C., Lopes-dos-Santos, V., Bacelo, J., Tort, A.B.L., 2019. Spike sorting with Gaussian mixture models. Sci. Rep. 9. https://doi.org/10.1038/s41598-019-39986-6

Steinmetz, N.A., Koch, C., Harris, K.D., Carandini, M., 2018. Challenges and opportunities for large-scale electrophysiology with Neuropixels probes. Curr. Opin. Neurobiol. 50, 92–100. https://doi.org/10.1016/J.CONB.2018.01.009

Torebjork, H.E., Hallin, R.G., 1974. Responses in human A and C fibres to repeated electrical

intradermal stimulation. J. Neurol. Neurosurg. Psychiatry 37, 653–664. https://doi.org/10.1136/jnnp.37.6.653

Vallbo, Å.B., 2018a. Microneurography: how it started and how it works. J. Neurophysiol. 120, 1415–1427. https://doi.org/10.1152/jn.00933.2017

Vallbo, Å.B., 2018b. Microneurography: how it started and how it works. J. Neurophysiol. 120, 1415–1427. https://doi.org/10.1152/jn.00933.2017

Weidner, C., Schmelz, M., Schmidt, R., Hansson, B., Handwerker, H.O., Torebjörk, H.E., 1999. Functional attributes discriminating mechano-insensitive and mechano- responsive C nociceptors in human skin. J. Neurosci. 19, 10184–10190. https://doi.org/10.1523/jneurosci.19-22-10184.1999

Zimmermann, K., Hein, A., Hager, U., Kaczmarek, J.S., Turnquist, B.P., Clapham, D.E., Reeh, P.W., 2009. Phenotyping sensory nerve endings in vitro in the mouse. Nat. Protoc. 4, 174–196. https://doi.org/10.1038/nprot.2008.223